ERNEST ORLANDO LAWRENCE
BERKELEY NATIONAL LABORATORY

LHC Kicker Beam-Impedance Calculation

Glen Lambertson

**Accelerator and Fusion
Research Division**

October 1998

DISCLAIMER

DISCLAIMER

Portions of this document may be illegible in electronic image products. Images are produced from the best available original document.

LHC Kicker Beam-Impedance Calculation*

Glen Lambertson
Lawrence Berkeley National Laboratory
University of California
Berkeley, California 94720

Abstract

Longitudinal and transverse beam impedances are calculated for
the injection kickers designed for use in the CERN large hadron col-
lider. These combine the contributions of a ceramic beam tube with
conducting stripes and a traveling-wave kicker magnet. The results
show peak impedances of 1300 ohm longitudinal and 8 MΩ/m trans-
verse for four units per ring.

Introduction

The injection kickers designed for the CERN LHC consist of four units for
each beam [1]; each of these has a C-magnet with a single-turn coil and
a beam tube of alumina ceramic shown schematically in Fig. 1. We shall
calculate the beam impedances of one of these assemblies. The winding has
added distributed capacitance to reduce its characteristic line impedance Z_c.
On the inner surface of the beam tube are thirty stripes of deposited metal
which I call the liner. Each of these stripes connects to the metal beam tubes
at its ends through parallel R-C circuits. These stripes and the surrounding

1

magnet present to the beam image currents 31 parallel paths; the impedance of this network is the beam impedance. For completeness I have included most of the components but in some cases with simplifying assumptions. Where the final, to be fabricated, parameters are not known, I have used estimated example values.

The portion I of the image current $-I_B$ that flows along the liner stripes reduces the net current $I_M = I_B + I_2$ that develops voltage across the impedance Z_M of the magnet. In detail, the voltage induced in a stripe from coupling to the magnet depends upon the position of the stripe in the magnet gap. The consequent differences between currents in the strips is a complexity that I shall ignore in order to simplify the analysis of the coupled circuits. With all stripes equivalent, we can calculate a liner impedance Z_L; the beam impedance Z_B is then the parallel combination of Z_L and Z_M,

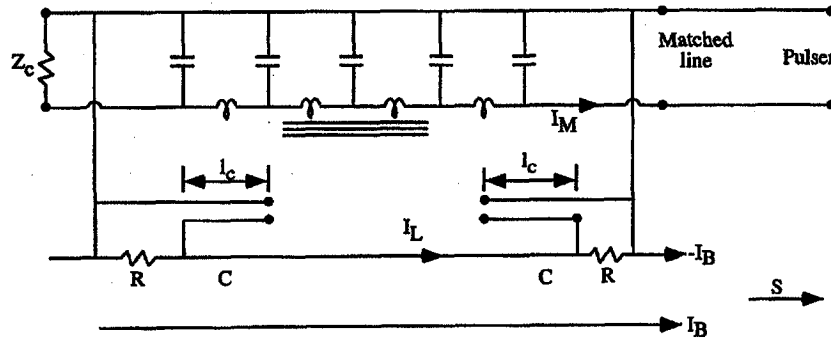$$\frac{1}{Z_B} = \frac{1}{Z_L} + \frac{1}{Z_M} \tag{1}$$

Figure 1: Schematic of circuits in kicker magnet with liner. I_B is the beam current.

Liner Longitudinal Impedance

To provide 600 pF capacitance at each end of the 30 stripes the ceramic tube is metallized on the outside for about 0.4 meter. This overlaps the ends of

the inside stripes by, I estimate, about 0.28 meter. Each stripe is connected to the outer sleeve by a 5 kilo-ohm resistor. Parameters of the liner are given in Table 1.

Table 1: Liner Parameters

Tube inner radius	b	21 mm
Ceramic well thickness		4 mm
Relative dielectric constant	ϵ_r	9
Number of stripes	N	30
Length of stripe	ℓ_s	3540 mm
Width of stripe	w	4 mm
Space between stripes	a/2	4 mm
Capacitance (30 stripes, one end)	C	600 pF
Length of capacitor line	ℓ_c	280 mm
Phase velocity along capacitor	v_c	$\sim 0.385\ c$
Resistance (5000/30)	R	169 ohm

As sketched in Fig. 1, the capacitor is in the form of a short open-ended transmission line. This presents impedance

$$\frac{1}{j\frac{Cv_c}{\ell_c}\tan\frac{\omega\ell_c}{v_c}}$$

Resonances with high impedance appear in this at multiples of 206 MHz. The shunting resistors limit the peak impedance to 167 ohms at each end.

We expect some inductance from the striped wall. The effect of the striping is small but it is calculated in Appendix 1. Combining the resistors, the capacitors, and the stripes, we get for the total impedance

$$Z_L = \frac{2}{\frac{1}{R} + j\frac{Cv_c}{\ell_c}\tan\frac{\omega\ell_c}{v_c}} + j\frac{\omega\mu_0\ell_s}{2\pi N}\frac{\epsilon_r - 1}{\epsilon_r + 1}\left(csc\frac{\pi w}{2a}\right) \tag{2}$$

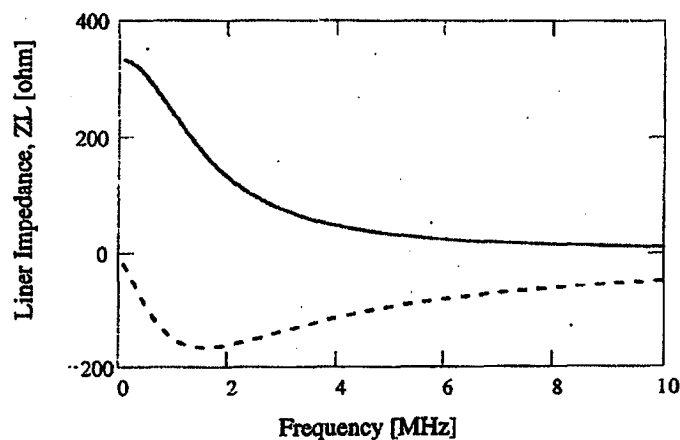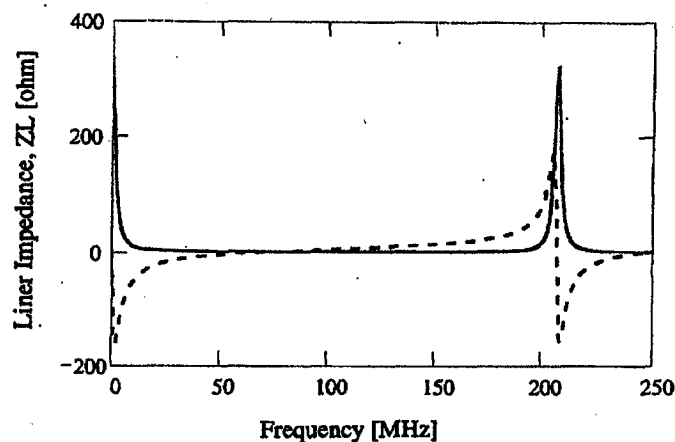This is plotted in Figure 2.

3

Fig. 2a

Fig. 2b

Figure 2: Impedance of the liner. Solid — ReZ_L[Ohm]. Dashed — ImZ_L[ohm].

Impedance from the Magnet

A sketch of the magnet aperture in shown in Fig. 3; the liner is not shown. Currents I_M that excite the magnet flow on the outside of the liner stripes. When the beam is off-center, the non-uniform distribution of currents drives

4

the magnet as if from a current at the displaced beam positron. Here in Fig. 2 the exciting current is shown simply as localized at distance y above the center. Having the longitudinal impedance as a function of position y will be used in calculating the transverse impedance. The current I_M couples inductively to the yoke and to the current it induces in the winding; each contributes to the impedance. The parameters of the magnet that we shall use are given in Table 2.

The coupling to the yoke is found assuming image-forming currents in the windings but no circulating induced current. In Appendix II the flux between aperture center and the grounded conductor is calculated by summing images in the aperture walls. In addition, there is in the 6 mm-space between the stripes and ground the direct field $\mu_0 I_M/2\pi y$. Also here are capacitive electric fields that reduce the beam impedance. But the currents I_M propagate slowly because of interaction with the magnet and the presence of the ceramic tube. These details determine the degree of cancellation between inductive and capacitive impedances. Rather than imperfectly analyze these factors, I note that the flux in the 6 mm is only about one eighth that from images and I accept the error in ignoring the effects of this space. The result is an
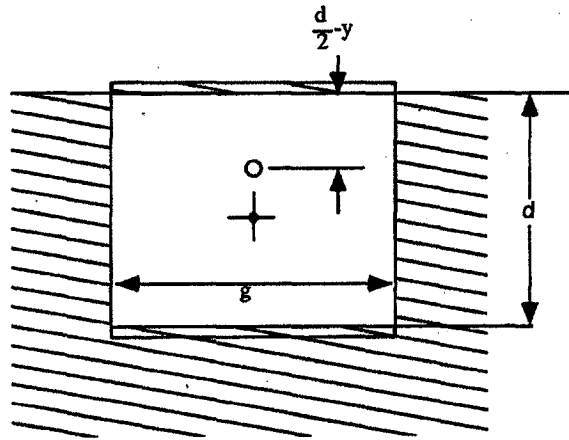

Figure 3: Magnet aperture with I_M shown at distance y from center toward the grounded winding

Table 2: Magnet Parameters

Length	ℓ	2657 mm
Aperture gap	g	54 mm
Aperture width	d	54 mm
Winding inductance per unit length ($=\mu_o$)	L'	1.25×10^{-6} Hy/m
Winding line-impedance	Z_c	5 ohm
Phase velocity (Z_c/L')	v	4×10^6 m/sec
Drive line delay (example)	τ	0.233 μsec

impedance from the yoke of

$$Z_Y = j\omega\mu_0\ell\,0.317 \tag{3}$$

For reference here we note that with the square aperture, $\mu_0\,\ell$ is the total inductance of the magnet.

The winding, as sketched in Fig. 1, is terminated at the upstream end by its characteristic line impedance Z_c and at the downstream end it connects to a cable of like impedance that is open at the pulser switch. In an increment of length ds, the mutual inductance between beam and winding is

$$M'ds = \mu_0 \frac{\frac{d}{2} - y}{g}\,ds = \frac{L'}{2}\left(1 - \frac{2y}{d}\right)\,ds \tag{4}$$

where L' is the inductance per unit length. At axial position s_1, the electric field induced at the winding is

$$E = -\,j\omega M' I_M e^{-jk_0 s_1} \tag{5}$$

Because in the low-frequency range where the magnet's influence is strong, the phase factor $k_0\,\ell$ is not large, we shall discard this factor in what follows. The field at s_1 launches increments of current that propagate at speed v downstream and upstream.[2] At any position s, the increments are

$$dI = \frac{E}{2Z_c}\,ds_1\,e^{-jk(s-s_1)} \text{ for } s > s_1$$

$$dI = \frac{E}{2Z_c}\,ds_1\,e^{jk(s-s_1)} \text{ for } s < s_1 \tag{6}$$

where $k = \omega/v$. Integrating over s_1 from $-\ell/2$ to $+\ell/2$ we obtain at s

$$I = \frac{E}{jkZ_c} \left(1 - e^{-j\frac{k\ell}{2}} \cos ks\right) \tag{7}$$

At the upstream end this current is absorbed by the load Z_c. At the downstream end, it is reflected by the unterminated cable, which has delay-length τ. The reflection arrives phase-delayed by $2\omega\tau$ and inverted. Combining this reflected current with I above, we obtain the total induced winding current

$$I(s) = \frac{E}{jkZ_c} \left[1 - e^{-j\frac{k\ell}{2}} \cos ks - e^{-j2\omega\tau} \left(1 - e^{-j\frac{k\ell}{2}} \cos \frac{k\ell}{2}\right) e^{jk(s-\ell/2)}\right]$$

Simplify by inserting $Z_c = L'v$ and M' and E from Eq. 4 and Eq. 5 and let $\frac{k\ell}{2} = \theta$:

$$I(s) = -\frac{I_M}{2} \left(1 - \frac{2y}{d}\right) \left[1 - e^{-j\theta} \cos ks + e^{-j2\omega\tau} e^{jks} j \sin \theta\right] \tag{8}$$

To obtain the beam voltage in one passage we integrate $-j\omega M' I(s)$ over the length, again neglecting the beam phase factor $k_o s$:

$$V = \frac{I_M Z_c}{2} \left(1 - \frac{2y}{d}\right)^2 \left[j\left(\theta - e^{-j\theta} \sin \theta\right) - e^{-j2\omega\tau} \sin^2 \theta\right] \tag{9}$$

This voltage contributes $-V/I_M$, which combines with Z_Y from Eq. 4 to give for the magnet alone the beam impedance at $y = 0$

$$Z_M = \frac{Z_c}{2} \left[0.268\, j\theta + e^{-j\theta} j \sin \theta + e^{-j\omega\tau} \sin^2 \theta\right] \tag{10}$$

This is shown in Fig. 4. The currents induced in the winding provide the resistive impedance and reduce the inductance.

Total Longitudinal Impedance

The parallel combination of Z_L and Z_M (Eq. 1) give the total impedance Z_B shown in Fig. 5. We see the capacitor's resonance at 206-MHz multiples but a second peak appears at 19 MHz. This is the resonance between the liner's capacitance and the magnet inductance. All these peaks are limited to 330 ohm by the series resistance of the liner.
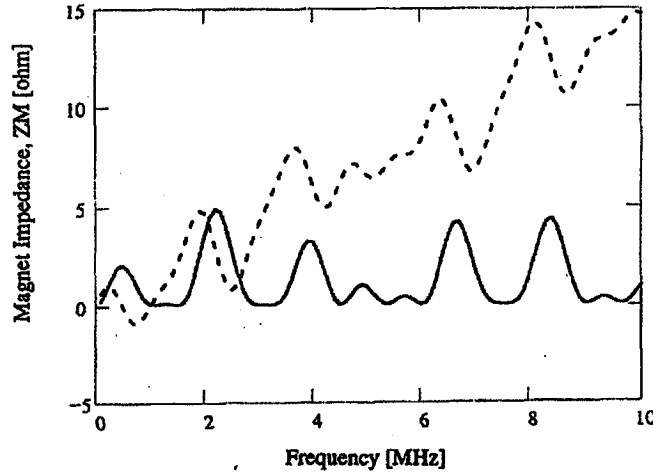
Figure 4: Impedance of the magnet. Solid — ReZ_M [ohm]. Dashed — ImZ_M [ohm].

Transverse Impedance from the Liner

Because the liner is azimuthally symmetric about the beam current, its transverse impedance acting on current I_L is given in terms of Z_L from Eq. 3 as

$$Z_{Lt} = \frac{2c}{\omega b^2} Z_L \qquad (11)$$

Transverse Impedance from the Magnet

For the magnet we must calculate separately the transverse effect of (1) the field from images in the aperture walls and (2) the interaction through induced winding currents.

In Appendix II, the image currents are shown to give zero y-impedance. For the x-component, we have, from Appendix II,

$$Z_{Yx} = j \frac{\ell c}{I} \frac{\partial \beta_y}{\partial x_0} = j \frac{\mu_0 c \ell}{g^2} (0.019) \qquad (12)$$
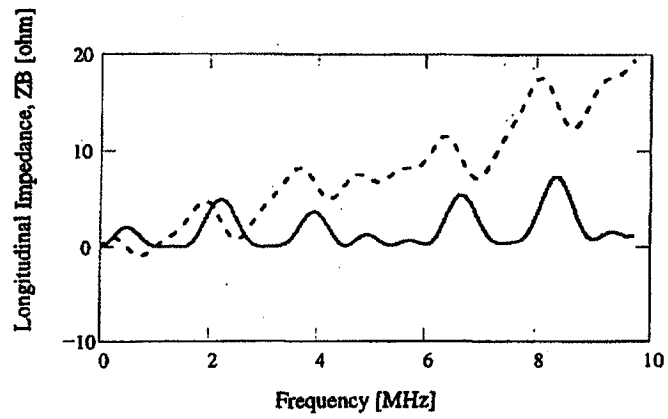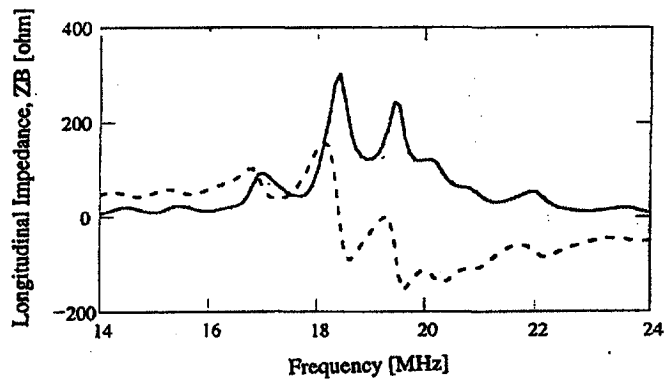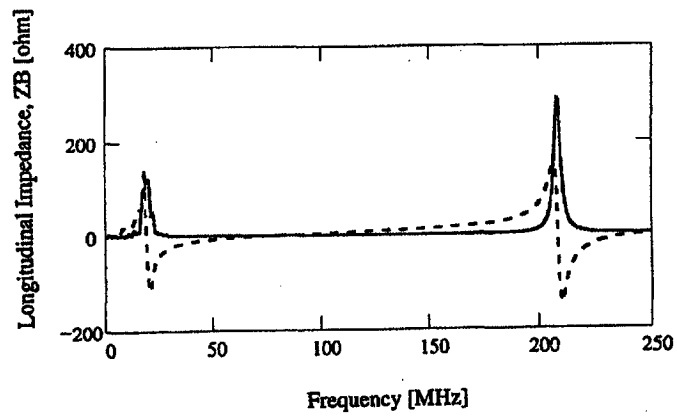
8

Fig. 5a

Fig. 5b

Fig. 5c

Figure 5: Total longitudinal impedance. Solid — ReZ_B [ohm]. Dashed — ImZ_B [ohm].

9

To obtain the transverse effect of the induced currents, we may use the Panofsky-Wenzel theorem applied to the transverse impedance:

$$Z_y = \frac{c}{\omega \Delta y} \frac{2 Z_{\parallel}}{2y} \tag{13}$$

Here the partial derivative relates transverse to longitudinal fields while Δy is a shift in the position of I_M. In Eq. 8 the factor $\left(1 - \frac{2y}{d}\right)$ was introduced once to give the dependence on position of I_M and a second time to show the observer's position. Therefore in Eq. 13 these factors introduce $(2/d)^2$. The transverse impedances from the magnet are

$$Z_{My} = \frac{c}{\omega} \frac{2}{d^2} Z_c \left[-j\, \theta + j\, e^{-j\theta}\, sin\theta + e^{-j2\omega\tau}\, sin^2\, \theta \right] \tag{14}$$

$$Z_{Mx} = \frac{\mu_0 c\, \ell}{g^2}\, (j\, 0.019) = \frac{c}{\omega} \frac{2}{g^2} Z_c\, (j\, 0.019\, \theta) \tag{15}$$

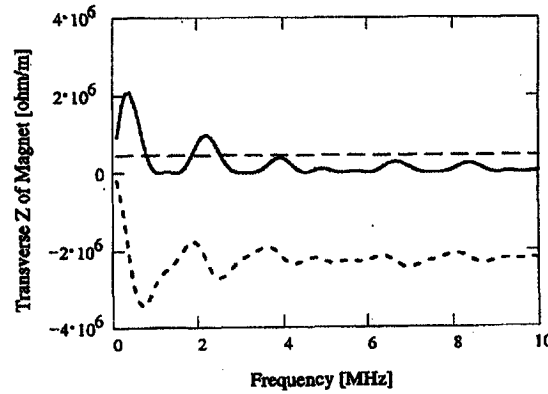These contributions from the magnet are shown in Fig. 6.

Figure 6: Horizontal (x) and vertical (y) impedances from the magnet. Solid — ReZ_{my} [ohm/m]. Short dash — ImZ_{my} [ohm/m]. Long dash — ImZ_{Mx} [0.1 ohm/m]
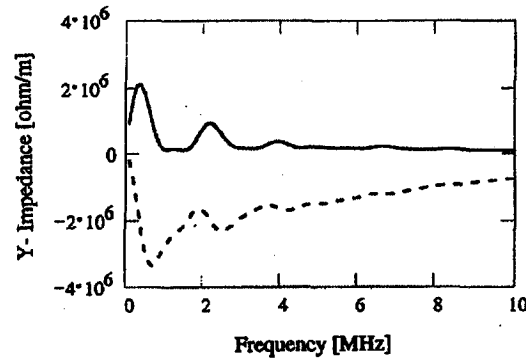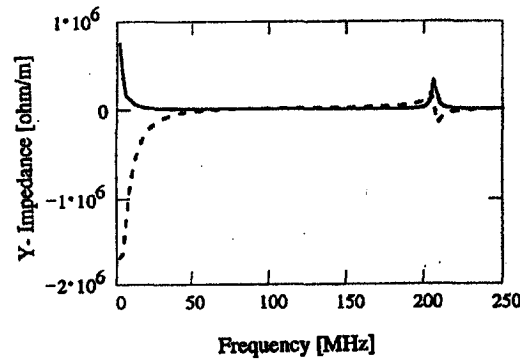
10

Fig. 7a

Fig. 7b

Figure 7: Total vertical impedance. Solid — ReZ_y[ohm/m]. Dashed — ImZ_y [ohm/m].

Total Transverse Impedance

With magnet and liner contributions combined in parallel, the total impedances are plotted in Figs. 7 and 8. A peak in Z_x appears at 44 MHz where Z_{Lx} and Z_{Mx} resonate. The values of these at orbital frequency are

$$Z_x(f_0) = 0.287 + j\,4.294 \times 10^4 \; ohm/m$$
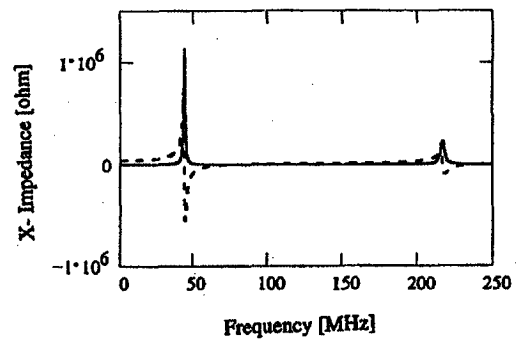
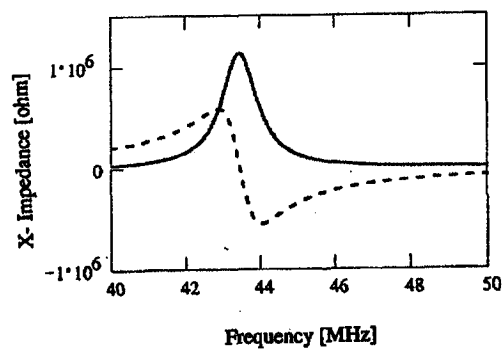$$Z_y(f_0) = 1.06 \times 10^5 - j\,2.58 \times 10^3 \; ohm/m$$

(16)

11
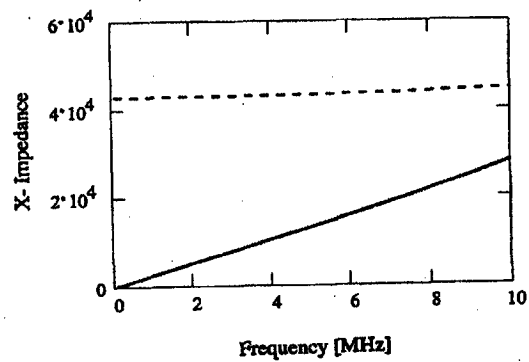
Figure 8: Total horizontal impedance. Solid — ReZ_x[ohm/m]. Dashed — ImZ_x [Ohm/m]. In Fig. 8(c), ReZ_x is plotted in 0.01 ohm/m.

12

References

[1] L. Ducimetière, U. Jansson, G. H. Schröder, E. B. Vossenberg, M. J. Barnes, G. D. Wait, "Design of the Injection Kicker Magnet System for CERN's 14 TeV Proton Collider LHC," 10th IEEE Pulsed Power Conference, Albuquerque, NM, July 10 - 13, 1995.

[2] G. Nassibian, "The Low Frequency Beam Impedance of Matched Travelling Wave Kickers," CERN/PS 84-25, Aug. 1984.

[3] W. R. Smythe, <u>Static and Dynamic Electricity</u>, McGraw Hill, New York, 1939, p. 89.

Appendix I

Impedance of Striped Wall

In comparison with a continuous conductor on the beam tube wall, the N stripes alter the local fields introducing added inductances and reduced capacitance. Once these are known, the effect on the beam impedance is found by the usual procedure of applying $\nabla \times E = -\partial B/\partial t$ in a short region between beam and wall.

In Fig. 9 with beam current $I = Q'c$ that varies as $e^{j(\omega t - k_o s)}$, this procedure gives

$$\frac{\partial V_r}{\partial \delta} + E_s = -j\omega\phi' \tag{17}$$

with primes denoting values per unit s. We let

$$V_r = Q'\left(\frac{1}{C'} + \Delta\frac{1}{C'}\right) \text{ and } \phi' = I(L' + \Delta L') \tag{18}$$

where L' and $\frac{1}{C'}$ are the usual continuous-wall values to which are added $\Delta L'$ and $\Delta\frac{1}{C'}$, from the striped wall.
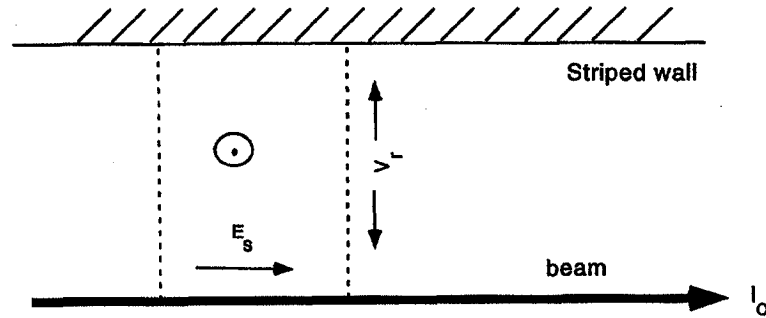

Figure 9: Fields between beam current and wall

For E_s we obtain

$$E_s = -j\omega I\left[\left(L' - \frac{1}{c^2 C'}\right) + \left(\Delta L' - \frac{1}{c^2}\Delta\frac{1}{C'}\right)\right] \tag{19}$$

14

The term with an unmodified L' and C' vanishes leaving

$$\Delta Z_L = -\frac{E_s \ell_s}{I_0} = j\omega \ell_s \left(\Delta L' - \frac{1}{c^2} \Delta \frac{1}{C'}\right) \qquad (20)$$

as the contribution to the beam impedance from the striped region of length ℓ_s.

To evaluate ΔZ_L we examine the fields near one conducting strip of width a on the ceramic wall at radius b. Because b/a is about 10, we approximate the curved geometry of the cylinder with rectangular. And because the fields will not extend far into the ceramic, we let the ceramic extend to $y = +\infty$.

We shall combine uniform fields (Fig. 10a) with those of a charged strip (Fig. 10b) to obtain the configuration that can terminate the fields from a beam current. In Fig. 10a with no charge on the strip, a uniform electric field E_1, in vacuum will continue in the ceramic at strength E_1/ϵ_r. In Fig. 10b with a charged strip, one may have the fields in ceramic and in vacuum equal and symmetric. This is the case because there is no field normal to the
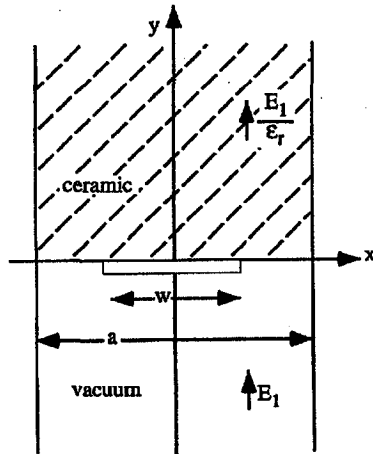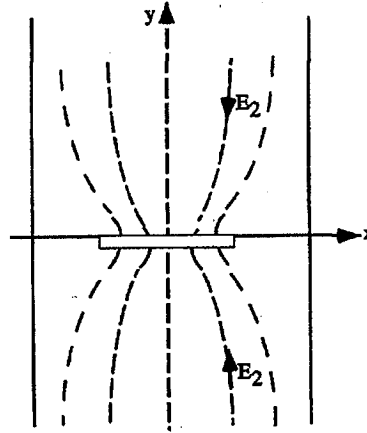

Figure 10a

Figure 10b

Figure 10: Region near conducting strip. (10a) Uncharged strip with uniform fields. (10b) Charged strip with symmetric fields in ceramic and vacuum.

15

ceramic surface. Let the fields as y approaches $\pm \infty$ be $\mp E_2$. This would arise from a charge density per unit length s along the strip on the vacuum side of

$$Q' = -\epsilon_0 E_2 a \tag{21}$$

and ϵ_r times that density on the side facing ceramic.

The total charge density per sector of width a is then

$$Q' = -\epsilon_o E_r a (1 + \epsilon_r) \tag{22}$$

The complex potential $W = U + jV$ for this field is given in Dwight (ref.) as

$$W_2(z) = E_2 \frac{a}{\pi} sin^{-1} \frac{sin \frac{\pi z}{a}}{sin \frac{\pi w}{2a}} \tag{23}$$

For the strip to terminate a field from the vacuum-side, add a field E_1 and require that at $y = +\infty$

$$\frac{E_1}{\epsilon_r} - E_2 = 0 \tag{24}$$

making the field at large negative y be

$$E_0 = E_1 + E_2 = (1 + \epsilon_r) E_2 \tag{25}$$

The potential function for this combined field is $W(z)$ with $E_1 \frac{z}{\epsilon_r}$ subtracted, i.e.

$$W(z) = \frac{E_0}{1 + \epsilon_r} \left[-z + \frac{a}{\pi} sin^{-1} \frac{sin \frac{\pi z}{a}}{sin \frac{\pi w}{2a}} \right] \tag{26}$$

We can now calculate $\Delta \frac{1}{C'} = \Delta V / Q' N$ where the added potential ΔV is found as the change in W from $y = 0$ to $y = \infty$.

$$j \Delta V = lim_{y \to \infty} \frac{E_0}{1 + \epsilon_r} \left[-jy + \frac{a}{\pi} sin^{-1} \frac{j \; sinh \frac{\pi y}{a}}{sin \frac{\pi w}{2a}} \right]$$

$$\Delta V = \frac{E_0}{1 + \epsilon_r} \frac{a}{\pi} \left(csc \frac{\pi w}{2a} \right) \tag{27}$$

16

Using $Q' = \epsilon_0 E_0 a$ we get for N stripes

$$\Delta\frac{1}{C'} = \frac{1}{N\pi\epsilon_0(1+\epsilon_r)} \ln\left(csc\,\frac{\pi w}{2a}\right) \tag{28}$$

To calculate $\Delta L'$, we can interpret W as the magnetic potential $MMF + j$ flux, letting

$$W(Z) = \frac{B_0}{2}\left[-z + \frac{a}{\pi}\,sin^{-1}\frac{sin\,\frac{\pi y}{a}}{sin\,\frac{\pi w}{2a}}\right] \tag{29}$$

which would terminate the magnetic field from a current $I/N = B_0 a/\mu_0$ in the sector. The added inductance is found, as for Δ/C', to be

$$\Delta L' = \frac{\mu_0}{N2\pi}\,\ln\left(csc\,\frac{\pi w}{2a}\right) \tag{30}$$

Using Eqs. 20, 28, and 30 we can write ΔZ_L as

$$\Delta Z_L = j\,\frac{\omega\mu_0\ell_s}{2\pi N}\,\frac{\epsilon_r - 1}{\epsilon_r + 1}\,\left(csc\,\frac{\pi w}{2a}\right) \tag{31}$$

For our liner this amounts to an inductance of only 6.54 picohenry.

Appendix II

Field from Images in the Yoke

We shall need the magnetic field from the beam current I that arises from its images in the magnetic walls at $x = \pm g/2$ and in the conductor surfaces at $y = \pm d/2$. In the square aperture, $d = g$. Place the current a distance y_0 above the aperture center and calculate the x-directed filed at points $x = 0$, $y = y$.

In Figure ?? the aperture is shown surrounded by example current images, the positions of which are sketched relative to a grid of points spaced g or d apart and designated by integers m and n. Positive images, and the beam current, are represented by $o's$ and negatives by $x's$.
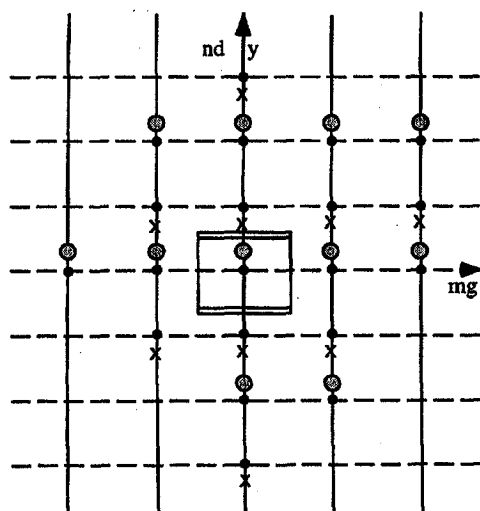

Figure 11: Examples of beam-current images surrounding the magnet aperture. The beam is shown displaced upward from the aperture center.

18

Summing images over a grid $2M$ by $2N$ and letting $y = ad$, $y_o = a_o d$, we have the field B_x

$$B_x = \frac{\mu_0 I}{g} \left[-\frac{1}{2} + \frac{1}{\pi} \sum_{n=1}^{N} \frac{(-1)^n \ (a - (-1)^n a_0)}{n^2 \ - \ (a - (-1)^n a_0)^2} \ . \right.$$
$$\left. + \frac{1}{\pi} \sum_{m=1}^{M} \sum_{n=1}^{N} \frac{(-1)^n \ (n - a + (-1)^n a_0)}{m^2 \ - \ (n - a + (-1)^n a_0)^2} \right] \qquad (32)$$

The term "-1/2" is the offset caused by the open side of the C-magnet. The numerical sum of this equation gives a result that is approximately

$$B_x = \frac{-\mu_0 \ I}{g} \ (0.5 \ + 0.536 \ y/d) \qquad (33)$$

and the flux per unit length between $y = 0$ and $d/2$ is $-0.317 \ \mu_0 \ I$.

For calculating the y transverse impedance, one needs the gradient of B_x with respect to y_0 at $y = 0$. This was calculated from the expression in Eq. 32. The result is zero, which can also be seen analytically from the functions of Eq. 32.

Proceeding in a similar way to obtain the y-directed field from current displaced by x_0, we obtain

$$\frac{\partial B_y}{\partial x_0} = \frac{\mu_0 I}{\pi g^2} \left[\sum_{m=1}^{M} \frac{(-1)^m}{m^2} \ + \ \sum_{m=-M}^{M} \sum_{n=1}^{N} \frac{(-1)^m \ (n^2 \ - \ m^2)}{m^2 \ - \ (n^2 \ + \ m^2)^2} \right] \qquad (34)$$

This has the numerical value $0.019 \ \mu_0 I/g^2$.